# Encapsulation of FITC to monitor extracellular pH: a step towards the development of red blood cells as circulating blood analyte biosensors

**Sarah C. Ritter,[1] Mark A. Milanick,[2] and Kenith E. Meissner[1,*]**

[1]*Department of Biomedical Engineering, Texas A&M University, College Station, TX 77843, USA*
[2]*Department of Medical Pharmacology and Physiology, University of Missouri, Columbia, MO 65211, USA*
** kmeissner@tamu.edu*

**Abstract:** A need exists for a long-term, minimally-invasive system to monitor blood analytes. For certain analytes, such as glucose in the case of diabetics, a continuous system would help reduce complications. Current methods suffer significant drawbacks, such as low patient compliance for the finger stick test or short lifetime (i.e., 3–7 days) and required calibrations for continuous glucose monitors. Red blood cells (RBCs) are potential biocompatible carriers of sensing assays for long-term monitoring. We demonstrate that RBCs can be loaded with an analyte-sensitive fluorescent dye. In the current study, FITC, a pH-sensitive fluorescent dye, is encapsulated within resealed red cell ghosts. Intracellular FITC reports on extracellular pH: fluorescence intensity increases as extracellular pH increases because the RBC rapidly equilibrates to the pH of the external environment through the chloride-bicarbonate exchanger. The resealed ghost sensors exhibit an excellent ability to reversibly track pH over the physiological pH range with a resolution down to 0.014 pH unit. Dye loading efficiency varies from 30% to 80%. Although complete loading is ideal, it is not necessary, as the fluorescence signal is an integration of all resealed ghosts within the excitation volume. The resealed ghosts could serve as a long-term (>1 to 2 months), continuous, circulating biosensor for the management of diseases, such as diabetes.



**OCIS codes:** (280.0280) Remote sensing and sensors; (280.4788) Optical sensing and sensors; (160.2540) Fluorescent and luminescent materials; (170.1470) Blood or tissue constituent monitoring

## References and links

1. R. J. McNichols and G. L. Coté, "Optical glucose sensing in biological fluids: an overview," J. Biomed. Opt. **5**(1), 5–16 (2000).
2. M. S. D. Agus, J. L. Alexander, and P. A. Mantell, "Continuous non-invasive end-tidal CO2 monitoring in pediatric inpatients with diabetic ketoacidosis," Pediatr. Diabetes **7**(4), 196–200 (2006).
3. R. B. Easley, T. R. Johnson, and J. D. Tobias, "Continuous pH monitoring using the Paratrend 7 inserted into a peripheral vein in a patient with shock and congenital lactic acidosis," Clin. Pediatr. (Phila.) **41**(5), 351–355 (2002).
4. E. Garcia, T. J. Abramo, P. Okada, D. D. Guzman, J. S. Reisch, and R. A. Wiebe, "Capnometry for noninvasive continuous monitoring of metabolic status in pediatric diabetic ketoacidosis," Crit. Care Med. **31**(10), 2539–2543 (2003).
5. M. E. McBride, J. W. Berkenbosch, and J. D. Tobias, "Transcutaneous carbon dioxide monitoring during diabetic ketoacidosis in children and adolescents," Paediatr. Anaesth. **14**(2), 167–171 (2004).
6. J. D. Tobias, "Transcutaneous carbon dioxide monitoring in infants and children," Paediatr. Anaesth. **19**(5), 434–444 (2009).
7. J. P. Boyle, T. J. Thompson, E. W. Gregg, L. E. Barker, and D. F. Williamson, "Projection of the year 2050 burden of diabetes in the US adult population: dynamic modeling of incidence, mortality, and prediabetes prevalence," Popul. Health Metr. **8**(1), 29 (2010).

#146861 - $15.00 USD Received 2 May 2011; revised 17 Jun 2011; accepted 17 Jun 2011; published 22 Jun 2011

8. Centers for Disease Control and Prevention, "2011 National diabetes fact sheet" (U.S. Department of Health and Human Services, Centers for Disease Control and Prevention, 2011).
9. UK Prospective Diabetes Study (UKPDS) Group, "Intensive blood-glucose control with sulphonylureas or insulin compared with conventional treatment and risk of complications in patients with type 2 diabetes (UKPDS 33)," Lancet **352**(9131), 837–853 (1998).
10. The Diabetes Control and Complications Trial Research Group, "The effect of intensive treatment of diabetes on the development and progression of long-term complications in insulin-dependent diabetes mellitus," N. Engl. J. Med. **329**(14), 977–986 (1993).
11. Y. Ohkubo, H. Kishikawa, E. Araki, T. Miyata, S. Isami, S. Motoyoshi, Y. Kojima, N. Furuyoshi, and M. Shichiri, "Intensive insulin therapy prevents the progression of diabetic microvascular complications in Japanese patients with non-insulin-dependent diabetes mellitus: a randomized prospective 6-year study," Diabetes Res. Clin. Pract. **28**(2), 103–117 (1995).
12. U.S. Department of Health and Human Services, National Diabetes Education Program (NDEP). "Know your blood sugar numbers," National Diabetes Education Program publication NDEP-10 (2005).
13. American Diabetes Association, "Standards of medical care in diabetes--2011," Diabetes Care **34**(Suppl 1), S11–S61 (2011).
14. M. R. Burge, S. Mitchell, A. Sawyer, and D. S. Schade, "Continuous glucose monitoring: the future of diabetes management," Diabetes Spectrum **21**(2), 112–119 (2008).
15. J. Wagner, C. Malchoff, and G. Abbott, "Invasiveness as a barrier to self-monitoring of blood glucose in diabetes," Diabetes Technol. Ther. **7**(4), 612–619 (2005).
16. G. McGarraugh, "The chemistry of commercial continuous glucose monitors," Diabetes Technol. Ther. **11**(s1 Suppl 1), S17–S24 (2009).
17. I. Torres, M. G. Baena, M. Cayon, J. Ortego-Rojo, and M. Aguilar-Diosdado, "Use of sensors in the treatment and follow-up of patients with diabetes mellitus," Sensors (Basel Switzerland) **10**(8), 7404–7420 (2010).
18. T. Aye, J. Block, and B. Buckingham, "Toward closing the loop: an update on insulin pumps and continuous glucose monitoring systems," Endocrinol. Metab. Clin. North Am. **39**(3), 609–624 (2010).
19. H. Hanaire, "Continuous glucose monitoring and external insulin pump: towards a subcutaneous closed loop," Diabetes Metab. **32**(5), 534–538 (2006).
20. C. Wei, D. J. Lunn, C. L. Acerini, J. M. Allen, A. M. Larsen, M. E. Wilinska, D. B. Dunger, and R. Hovorka, "Measurement delay associated with the Guardian RT continuous glucose monitoring system," Diabet. Med. **27**(1), 117–122 (2010).
21. N. Wisniewski, F. Moussy, and W. M. Reichert, ""Characterization of implantable biosensor membrane biofouling," Fresenius'," J. Anal. Chem. **366**, 611–621 (2000).
22. G. Voskerician and J. Anderson, "Sensor Biocompatibility and Biofouling in Real-Time Monitoring," in *Wiley Encyclopedia of Biomedical Engineering*, (John Wiley & Sons, Inc., 2006).
23. M. Hamidi and H. Tajerzadeh, "Carrier erythrocytes: an overview," Drug Deliv. **10**(1), 9–20 (2003).
24. G. Schwoch and H. Passow, "Preparation and properties of human erythrocyte ghosts," Mol. Cell. Biochem. **2**(2), 197–218 (1973).
25. J. R. Deloach, "Carrier erythrocytes," Med. Res. Rev. **6**(4), 487–504 (1986).
26. G. M. Ihler and H. C.-W. Tsang, "Hypotonic hemolysis methods for entrapment of agents in resealed erythrocytes," Methods Enzymol. **149**, 221–229 (1987).
27. F. Pierigè, S. Serafini, L. Rossi, and M. Magnani, "Cell-based drug delivery," Adv. Drug Deliv. Rev. **60**(2), 286–295 (2008).
28. P. Seeman, "Transient holes in the erythrocyte membrane during hypotonic hemolysis and stable holes in the membrane after lysis by saponin and lysolecithin," J. Cell Biol. **32**(1), 55–70 (1967).
29. L. Rossi, S. Serafini, F. Pierigé, A. Antonelli, A. Cerasi, A. Fraternale, L. Chiarantini, and M. Magnani, "Erythrocyte-based drug delivery," Expert Opin. Drug Deliv. **2**(2), 311–322 (2005).
30. C. G. Millán, M. L. Marinero, A. Z. Castañeda, and J. M. Lanao, "Drug, enzyme and peptide delivery using erythrocytes as carriers," J. Control. Release **95**(1), 27–49 (2004).
31. M. Magnani, L. Rossi, A. Fraternale, M. Bianchi, A. Antonelli, R. Crinelli, and L. Chiarantini, "Erythrocyte-mediated delivery of drugs, peptides and modified oligonucleotides," Gene Ther. **9**(11), 749–751 (2002).
32. B. E. Bax, M. D. Bain, P. J. Talbot, E. J. Parker-Williams, and R. A. Chalmers, "Survival of human carrier erythrocytes in vivo," Clin. Sci. **96**(2), 171–178 (1999).
33. R. A. Schlegel, K. Lumley-Sapanski, and P. Williamson, "Single cell analysis of factors increasing the survival of resealed erythrocytes in the circulation of mice," Adv. Exp. Med. Biol. **326**, 133–138 (1992).
34. G. Gardos, "Akkumulation de kalium onen durch menschiche Blutkorperchen," Acta Physiol. Acad. Sci. Hung. **6**, 191–196 (1953).
35. N. V. B. Marsden and S. G. Ostling, "Accumulation of dextran in human red cells after haemolysis," Nature **184**(4687 Suppl 10), 723–724 (1959).
36. G. M. Ihler, R. H. Glew, and F. W. Schnure, "Enzyme loading of erythrocytes," Proc. Natl. Acad. Sci. U.S.A. **70**(9), 2663–2666 (1973).
37. U. Zimmerman, "Jahresbericht der kernforschungsanlage Jülich GmbH" (Nuclear Research Center, Jülich, 1973), pp. 55–58.
38. M. Hamidi, A. Zarrin, M. Foroozesh, and S. Mohammadi-Samani, "Applications of carrier erythrocytes in delivery of biopharmaceuticals," J. Control. Release **118**(2), 145–160 (2007).

#146861 - $15.00 USD Received 2 May 2011; revised 17 Jun 2011; accepted 17 Jun 2011; published 22 Jun 2011

39. R. Flower, E. Peiretti, M. Magnani, L. Rossi, S. Serafini, Z. Gryczynski, and I. Gryczynski, "Observation of erythrocyte dynamics in the retinal capillaries and choriocapillaris using ICG-loaded erythrocyte ghost cells," Invest. Ophthalmol. Vis. Sci. **49**(12), 5510–5516 (2008).
40. R. Azoui, J. L. Cuche, J. F. Renaud, M. Safar, and G. Dagher, "A dopamine transporter in human erythrocytes: modulation by insulin," Exp. Physiol. **81**(3), 421–434 (1996).
41. A. Carruthers, "Facilitated diffusion of glucose," Physiol. Rev. **70**(4), 1135–1176 (1990).
42. P. G. LeFevre, "Evidence of active transfer of certain non-electrolytes across the human red cell membrane," J. Gen. Physiol. **31**(6), 505–527 (1948).
43. O. Fröhlich and R. B. Gunn, "Erythrocyte anion transport: the kinetics of a single-site obligatory exchange system," Biochim Biophys Acta. **864**, 169–194 (1986).
44. J. Funder and J. O. Wieth, "Chloride transport in human erythrocytes and ghosts: a quantitative comparison," J. Physiol. **262**(3), 679–698 (1976).
45. H. Cao and M. D. Heagy, "Fluorescent chemosensors for carbohydrates: a decade's worth of bright spies for saccharides in review," J. Fluoresc. **14**(5), 569–584 (2004).
46. H. Fang, G. Kaur, and B. Wang, "Progress in boronic acid-based fluorescent glucose sensors," J. Fluoresc. **14**(5), 481–489 (2004).
47. P. S. B. Center, Donating Platelets, http://www.psbc.org/programs/platelets.htm.
48. P. K. Gasbjerg, P. A. Knauf, and J. Brahm, "Kinetics of bicarbonate transport in human red blood cell membranes at body temperature," J. Gen. Physiol. **108**(6), 565–575 (1996).
49. H. Bodemann and H. Passow, "Factors controlling the resealing of the membrane of human erythrocyte ghosts after hypotonic hemolysis," J. Membr. Biol. **8**(1), 1–26 (1972).

## 1. Introduction

Analysis of various blood parameters provides insight into critical aspects of a patient's physiological or biochemical state, thus providing information about organ function and disease status. Examples of important blood parameters include pH, catecholamines, and glucose, which at elevated levels is linked to diabetes [1]. Changes in blood pH accompany a variety of diseases, such as diabetic ketoacidosis and congenital lactic acidosis [2,3]. During treatment, it is critical to monitor blood pH, as the treatment itself may cause an overshoot of the set pH value [2,4–6]. Currently, the gold standard measurement for blood pH is sampling of arterial blood, which is both inconvenient and difficult, especially with infants and pediatric patients. A secondary method for estimating blood pH is measurement of transcutaneous $pCO_2$ or end tidal $CO_2$ levels. Although hourly samples are valuable, patients may experience rapid changes in blood pH and require immediate treatment. Thus, a long-term, continuous solution, e.g. a biosensor, is requisite for more complicated and serious conditions, such as diabetes or diabetic ketoacidosis.

The increasing prevalence of diabetes in the United States drives the demand for more effective solutions to control the disease and disease-associated complications. Although roughly 1 out of 10 adults have Type II diabetes today, a recent report by the CDC indicates that the number may rise to 1 out of 3 by 2050 [7]. Diabetes was ranked as the seventh leading cause of death in 2007 [8], costing an estimated $174 billion [7]. However, research has shown that maintaining proper blood sugar levels may prevent or delay diabetes-related complications [9–11]. The current standard for blood glucose monitoring, the finger stick test, provides only a small set (e.g., 3–7) of glucose measurements daily [12,13]. These discrete measurements fail to provide sufficient information about blood glucose trends throughout the day [14]. Furthermore, the invasiveness of this technique serves as an obstacle to proper control of blood glucose levels through self-monitoring [1,15]. Thus there is a demand for continuous, minimally-invasive sensors that provide glucose measurements that correlate to blood levels [15]. Because of this demand, glucose monitoring has become the most heavily researched application for biosensors.

Current research into continuous, minimally invasive glucose sensors focuses on systems that can be implanted subcutaneously, where the sensors are in continuous contact with the interstitial fluid. Multiple continuous glucose monitoring systems are commercially available, including Abbott's FreeStyle Navigator®, the DexCom™ STS®-7, and Medtronic's Guardian® Real-Time [16,17]. However, these systems are approved only for use along with the finger stick test and cannot be used alone to determine treatment methods [13]. These systems

#146861 - $15.00 USD Received 2 May 2011; revised 17 Jun 2011; accepted 17 Jun 2011; published 22 Jun 2011

measure glucose levels through an enzymatic reaction between glucose oxidase on the electrode and glucose in the interstitial fluid [14,17,18]. However, these systems require frequent calibrations with the standard finger stick test to account for variations in the reaction and diffusion kinetics [19]. Also, changes in the glucose levels of the interstitial fluid temporally lag those of the blood [14,17,18,20]. Generally, implanted sensors are viewed by the body as foreign objects, eliciting an immune response that ultimately leads to fibrous encapsulation and precludes proper, long-term functioning [21,22]. Although efforts to reduce *in vivo* biofouling of the continuous glucose monitoring sensors through application of specialized membranes have led to observed stability over the lifetime of the system [16,18], the implanted electrode still has an operational lifetime of only 3-7 days [14,16–18].

As an alternative, we propose that the sensing chemistry may be entrapped within red blood cells (RBCs) through the hypotonic dilution method. This method takes advantage of the RBC membrane's ability to reversibly swell in response to the osmolarity of the extracellular environment [23–26]. In this procedure, the RBCs are placed in a low osmolarity solution (i.e., lysis solution) at 0°C, which causes the membranes to swell and develop pores that are estimated to range from 10 to 500 nm [23,24,27,28]. While the pores are open, hemoglobin (Hb) and other molecules within the cell and fluorescent probes as well as salts in the lysis solution equilibrate. Once physiological osmolarity and temperature are restored, the pores reseal, entrapping the fluorescent probe. These carriers exhibit biodegradability and, as autologous cells, biocompatibility, thereby avoiding the deleterious effects of the immune system response [23,25,27,29–31]. Furthermore, resealed ghosts that have been returned to the body are able to circulate with a lifetime similar to normal RBCs [23,25,26,32,33]. Thus the sensors would have a lifetime of up to 120 days, depending upon the age of the RBCs at removal.

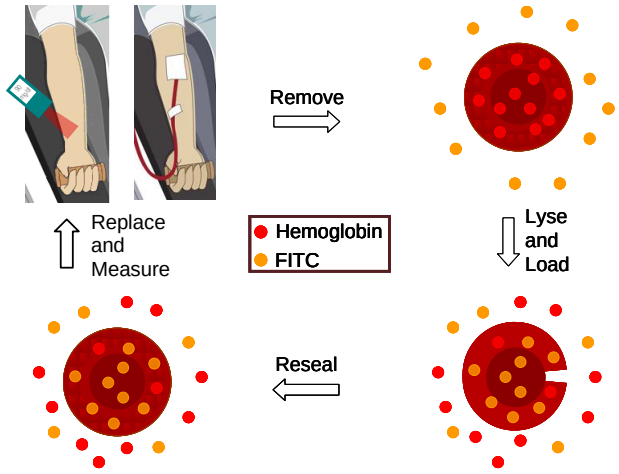


Fig. 1. Cartoon illustrating the RBC sensing platform concept. A small portion of blood is removed from the patient; the blood is washed, loaded with the analyte-sensitive fluorescent dye, resealed, and then transfused back into the patient. An excitation light source is then directed at the wrist; the emission from the resealed red cell ghosts is collected and converted into an analyte concentration. Clip art used with permission from Microsoft.

Efforts to entrap chemicals within RBCs began in the early 1950s with the successful encapsulation of ATP (as reviewed in [23,34]) and then, in 1959, various molecular weight dextrans [35]. In 1973, RBCs were first used as delivery vehicles for therapeutic agents by two independent groups [36,37]. Since these early studies, the advantages of RBCs (e.g., biocompatibility, biodegradability, long life time) have continued to drive the development of RBC carriers for delivery of biopharmaceuticals. Several excellent reviews on drug delivery using RBCs as biocompatible carriers are available [29,30,38]. In general, the means of

#146861 - $15.00 USD Received 2 May 2011; revised 17 Jun 2011; accepted 17 Jun 2011; published 22 Jun 2011

delivery may be either targeted or controlled drug release; the association between drug and RBC is either through encapsulation or membrane binding. Using these methods, a multitude of drugs, including those based on amino acids, proteins, and enzymes, have been investigated for their use in RBC delivery systems. Recently, ICG-loaded RBCs were used to study the hemodynamics of the retinal capillaries and choriocapillaris [39]. However, resealed red cell ghosts have yet to be explored as a means of monitoring analyte levels within the blood.

A unique property of RBCs that lends itself to biosensing is the existence of cell membrane transporters that provide a route to report on extracellular analyte and ion levels by monitoring intracellular levels. Examples of transported analytes include catecholamines, e.g., dopamine, noradrenaline, adrenaline [40]. Human RBCs transport glucose at a high rate [41,42] through the GLUT1 protein. RBC membranes of all species contain the chloride-bicarbonate exchanger, which is one of several pathways for ion transport [43]. In this work, we exploit this anion exchanger: the intracellular pH equilibrates to that of the extracellular solution in response to changes in the hydrogen ion activity of the RBC environment. Because the encapsulation method does not damage the exchanger, the extracellular pH can then be remotely monitored by measuring the fluorescence intensity of a pH-dependent probe encapsulated within the RBCs [44].

In this paper, we report on the proof-of-concept, platform technology based upon pH that may be expanded to monitor other circulating analytes, such as glucose. Although beyond the scope of the current work, it should be pointed out that visible-wavelength, glucose-sensitive fluorescent dyes are available [45,46]. Compared with pH dyes, however, dyes that are specific for glucose are traditionally more difficult to produce, due to the tendency for cross-reactivity with fructose. For *in vivo* work, the visible-wavelength, glucose-sensitive dyes can be adapted to emit in the NIR. The cartoon in Fig. 1 illustrates the envisioned concept in which a small portion (e.g., 1 unit or less) of a patient's blood would be removed, loaded with the analyte-sensitive fluorescent tag(s), and transfused back into the blood stream. This reintroduction process would be analogous to platelet donation, in which whole blood is removed, processed by a cell separating machine to remove platelets, and remaining components returned to the donor [47]. The resealed ghosts would then circulate for the remainder of the 120 day lifespan, reporting on analyte levels upon excitation by an external light source (e.g., laser diode).

## 2. Experimental section

### *2.1. Chemicals*

Lysis solution components ($MgCl_2$, EDTA, urea, and phosphate buffer), KCl, fluorescein 5(6)-isothiocyanate (FITC), glycylglycine, NaCl, and phosphate buffered saline (PBS) were purchased from Sigma Aldrich (St. Louis, MO). Anti-fluorescein/Oregon Green, rabbit IgG was purchased from Invitrogen (Carlsbad, CA). Whole sheep blood in citrate was purchased from Hemostat Laboratories (Dixon, CA). FITC was reacted with 4.3-fold excess glycylglycine at pH 9 to form the glycylglycine-FITC conjugate. All solutions were prepared with deionized water, adjusted to pH 7.4 with HCl and NaOH, and stored at 4°C.

### *2.2. Preparation of dye-loaded, resealed red cell ghosts*

In this preparation, RBCs are diluted ~10 times with a dye-containing solution. The resulting RBCs are termed "pink ghosts" due to the low final concentration of entrapped Hb (i.e., 10% of original). Low Hb ghosts were used in these initial experiments as Hb absorbance overlaps with the emission of the fluorescent probe. However, future work involves the incorporation of NIR fluorescent probes within high Hb ghosts, providing complete functionality of the RBC sensors *in vivo*.

Whole sheep blood was washed three times with 165 mM NaCl through centrifugation (10,000 x g, 3 minutes) to remove plasma proteins and leukocytes; washed, packed RBCs

#146861 - $15.00 USD Received 2 May 2011; revised 17 Jun 2011; accepted 17 Jun 2011; published 22 Jun 2011

were stored on ice until loading. The lysis solution (53 mls) consisted of 0.94 mM $MgCl_2$, 1.9 mM EDTA, 4.7 mM $KH_2PO_4$, 1 M urea, 0.947 mM glycylglycine, and 217 μM glycylglycine-FITC conjugate. This solution was stirred in a beaker surrounded by a salt water/ice mixture to maintain the temperature at 0°C for the loading procedure. Once the loading solution cooled to ~0°C, 5 mls of packed RBCs were added in a single injection. After 10 minutes, 5 mls of 1.65 M KCl were added to restore osmolarity. After another 10 minutes, the ghosts were transferred to a water bath at 37°C for 25 minutes to complete the resealing process. Free glycylglycine-FITC conjugate, Hb, residual leukocytes and RBC debris were removed via aspiration following three centrifugation cycles (10,000 x g, 8 minutes for first wash, 6 minutes for successive washes). Resealed ghosts not immediately used were stored at 4°C in 5 volumes of PBS.

*2.3. Sensor response and spectral data acquisition*

For pH experiments, 100 mM NaOH and HCl solutions were prepared in 165 mM NaCl to maintain the osmolarity of the local RBC environment. Resealed ghosts were added into room-temperature, isotonic NaCl until a sufficient fluorescence signal could be measured with the optical system. As ~90% of the Hb had been removed while making the resealed ghosts, 10 mM PBS was added to the resealed ghost solution to prevent large fluctuations in the extracellular pH.

Multiple optical systems were used to acquire the data presented in this paper:

*Dynamic data:* A frequency doubled Ti:sapphire laser (~15 mW, Mira 900, Coherent, Santa Clara, CA) served as the excitation source (λ ~440 nm) for the resealed ghosts ($\lambda_{ex,max}$ = 492 nm). A short-pass filter was placed just after the doubling crystal to remove remaining excitation light (880 nm). Fluorescence emission ($\lambda_{em,max}$ = 518 nm) was collected at 90° with a spectrograph (Acton SpectraPro 2300i, Princeton Instruments, Trenton, NJ) attached to a CCD camera (PIXIS 100, Princeton Instruments, Trenton, NJ). For time-course measurements, the fluorescence signal was integrated over 500–570 nm. The pH probe was placed in the extracellular solution to simultaneously monitor extracellular pH throughout the entire experiment. All pH data was collected through HyperTerminal on the PC.

*Static data:* Fluorescence emission was collected with a fluorimeter (PTI, Birmingham, NJ) using an excitation wavelength of 488 nm. For time-course measurements, the fluorescence emission of a single wavelength (i.e., 514 nm) was recorded for 20 to 30 seconds. Extracellular pH of the experimental solution of resealed ghosts was continuously measured with a pH probe (Orion 3 Star, Thermo Electron Corporation, Waltham, MA). Prior to data collection, anti-fluorescein antibody was added to the experimental solution to bind any free (i.e., extracellular) glycylglycine-FITC conjugate, quenching its contribution to the fluorescence signal. The fluorescence emission of a 1 ml sample of the experimental solution was recorded; the corresponding pH was recorded and the sample returned to the experimental solution. The pH of the experimental solution was adjusted, solution thoroughly mixed, and the measurements were repeated for several pH steps.

For the emission spectra of free glycylglycine-FITC conjugate and resealed ghosts presented in this paper, the samples were excited using a 488 nm argon ion laser (model 163-M12, 25 mW, Spectra-Physics Lasers, Santa Clara, CA). Fluorescence intensity was collected using the spectrograph/CCD camera setup described in the dynamic data section.

*Testing of sensor integrity:* To allow for comparison of intensity changes due to potential glycylglycine-FITC conjugate release, the fluorescence intensity value at 514 nm was collected for 30 seconds. The fluorescence contribution of extracellular glycylglycine-FITC conjugate was quenched by addition of an anti-fluorescein antibody. After the experimental time period of 30 minutes, the intensity value at 514 nm was collected for an additional 30 seconds. A second aliquot of the anti-fluorescein antibody was added and thoroughly mixed with the resealed ghosts. A third fluorescence time-based scan was recorded for 30 seconds for comparison.

#146861 - $15.00 USD Received 2 May 2011; revised 17 Jun 2011; accepted 17 Jun 2011; published 22 Jun 2011

## 3. Results and discussion

Fluorescein has a pKa of 6.4, leading to pH-dependent fluorescence emission over the range of pH 5 to 9. For the experiments presented here, the fluorescein derivative, FITC, was conjugated to glycylglycine, rendering a cell impermeant compound—a requisite for stable encapsulation. The spectra of resealed ghosts and free glycylglycine-FITC conjugate ($\lambda_{ex}$ = 488 nm) are compared in Fig. 2. Encapsulation of the fluorescent dye within the RBCs does not alter its emission curve.

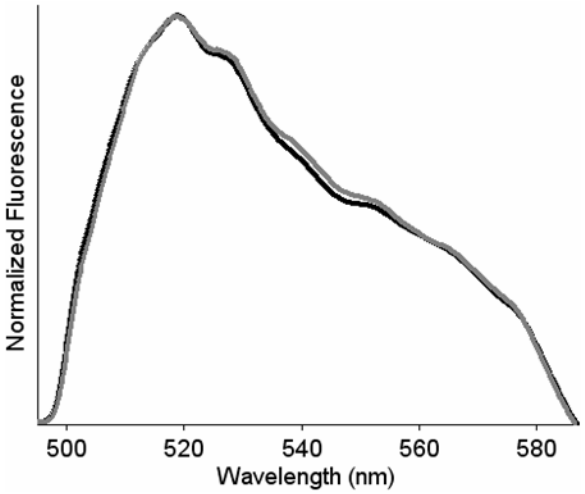


Fig. 2. Comparison of fluorescence spectra of resealed ghosts (black) and free glycylglycine-FITC conjugate (grey) show that emission characteristics of the two solutions are nearly identical.

To investigate the fluorescence intensity response to pH, acid or base was added in 1 to 5 µl aliquots to vary the pH of the resealed ghost environment between pH 6.5 and 8.5. The resealed ghost solution was thoroughly mixed after each addition. For the dynamic data, the fluorescence intensity and pH signals were allowed to plateau prior to each acid/base addition to ensure that the resealed ghosts had sufficient time to equilibrate. The response time, defined as the length of time required for the signals to reach a steady state value, was typically less than one minute. This response time most likely reflects the response time of the electronics and mixing time of the solution as the chloride-bicarbonate exchange system has a half time of less than 1 second at 37°C [48]. In the portion of the dynamic data shown in Fig. 3, fluorescence intensity (integrated from 500 to 570 nm) tracks extracellular pH throughout the pH range of interest. The two curves exhibit similar characteristics in response to pH changes, including directionality, drift, and signal change for corresponding changes in pH values. The sensors demonstrate reversibility across the pH range throughout the 25 minutes of optical interrogation time (e.g., two pH measurements of approximately 7, separated by 9 measurements over 16 minutes, had identical fluorescence intensity measurements within the experimental error of the system). This reversibility indicates that the optical system does not affect the membrane transporters or significantly photobleach the fluorescent probe. For the *in vivo* application of this sensor, the fluorescent probe would be subject to a significantly shorter excitation time (i.e., approximately 1 minute, or the response time of the sensor), and since the RBCs mix during circulation through the body, one would not expect that the same resealed ghosts would be found within the excitation volume for consecutive measurements. Thus, it is easy to envision that similar reversibility would be expected over the lifetime of the sensor.

#146861 - $15.00 USD Received 2 May 2011; revised 17 Jun 2011; accepted 17 Jun 2011; published 22 Jun 2011

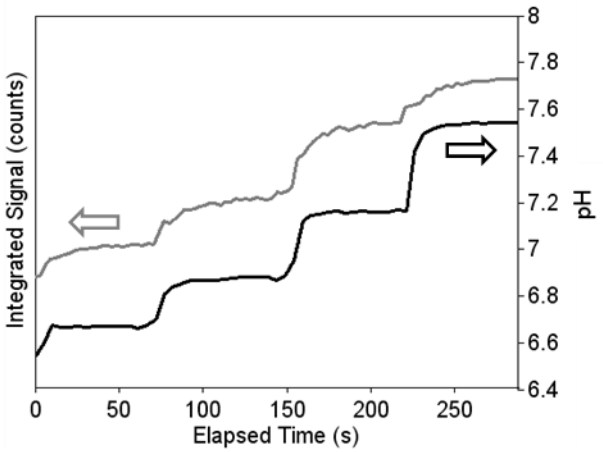


Fig. 3. A representative portion of a pH trial performed on the dynamic system. Fluorescence intensity (grey) of the intracellular pH-sensitive dye (FITC) tracks extracellular pH (black).

The potential release of glycylglycine-FITC conjugate was investigated to evaluate the integrity of resealed ghosts over the experimental time period (i.e., 30 minutes). In repeated testing, the extent of the subsequent decrease in the measured fluorescence signal due to the first antibody addition varied between 9% and 46%. This variation in the signal contribution is directly related to how well the resealed ghosts are washed at the end of the preparation step (i.e., removal of free glycylglycine-FITC conjugate); more thorough washing will lead to a decrease in the measured contribution of free glycylglycine-FITC conjugate. Measured fluorescence intensities before and after the second addition of anti-fluorescein antibody (after 30 minutes) were the same value within experimental error, indicating no significant amount of extracellular glycylglycine-FITC conjugate. Thus we assume the RBC membranes did not release glycylglycine-FITC conjugate during the pH experiments.

A pH trial performed on the static optical system is shown in Fig. 4. After quenching of the extracellular glycylglycine-FITC conjugate fluorescence contribution, extracellular pH was monitored with the fluorescence-based sensors. After each pH change, the fluorescence signal at 514 nm was monitored for 30 seconds to provide sufficient data to develop an average fluorescence signal at each pH; the pH was recorded for each pH step. This system shows similar reversibility as the dynamic system, indicating that this system does not negatively affect the RBC membranes.

After data collection, fluorescence intensity and corresponding pH values were selected for each signal plateau of the two pH trials (Fig. 3 and Fig. 4) to evaluate the sensor's ability to monitor extracellular pH as a function of the measured fluorescence intensity (Fig. 5). Both data sets were normalized at pH 7.4. The normalized sensitivity attained by the sensors was 0.44 per pH unit. For the dynamic system in Fig. 3, the normalized standard deviation was 0.002, leading to a resolution, defined as the smallest change in pH discernable from the fluorescence intensity data, of 0.014 pH unit. For the static system in Fig. 4, the normalized standard deviation was 0.0143, leading to a resolution of better than 0.1 pH unit. The decreased resolution of this system compared with the dynamic system is primarily attributed to electronic noise of the fluorimeter rather than to poor performance of the sensors since, for a sample of glycylglycine-FITC conjugate, the normalized standard deviation of the fluorimeter is 0.0149. The fluorescence intensity of the resealed ghosts shows a linear dependence between pH 6.5 and ~7.4. At higher pH values, the response becomes nonlinear, as expected for a dye with pK ~6.4. From these data, the pKs for the two resealed ghost sets were determined to be 6.65 and 6.59. These values vary slightly from the experimental pK of

#146861 - $15.00 USD Received 2 May 2011; revised 17 Jun 2011; accepted 17 Jun 2011; published 22 Jun 2011

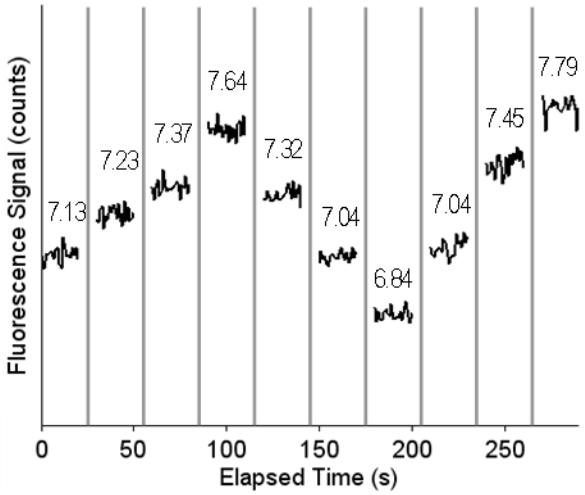


Fig. 4. Fluorescence intensity responds to pH changes using the static system in which extracellular glycylglycine-FITC conjugate fluorescence is quenched by the anti-fluorescein antibody. Each segment is the middle 15 seconds of a 30 second fluorescence monitoring period. The grey lines indicate discontinuous data. The average pH is directly above each segment.

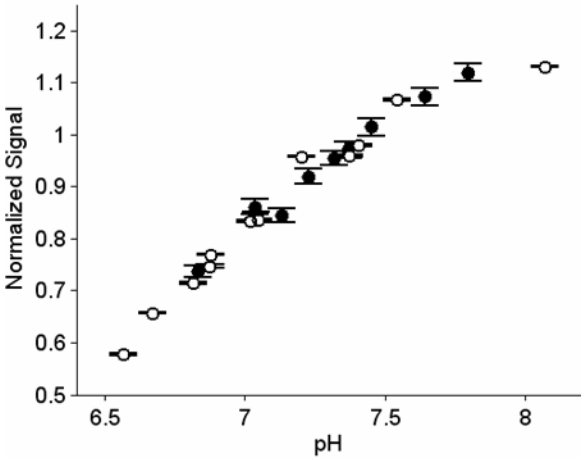


Fig. 5. Normalized fluorescence intensity as a function of pH for the pH trials shown above in Fig. 3 (○) and Fig. 4 (●). The two trials agree well. Error bars represent one standard deviation.

glycylglycine-FITC conjugate (pK 6.37), indicating that slight effects of the resealed ghost's cytosolic environment may exist. However, the resealed ghosts clearly track changes in extracellular pH over the physiological range.

The distribution of glycylglycine-FITC conjugate among the resealed ghosts was investigated through epifluorescence (λex = 488 nm, 60x objective) and bright-field phase microscopy (60x objective), as shown in Fig. 6. Comparison of same field images of resealed ghosts taken with each of these techniques indicates that approximately 50% of the resealed ghosts contained the fluorescent dye (unloaded RBCs are not observable in the fluorescent micrograph). This observation matches well with observations of Bodemann et al. indicating that ~60% of ghosts made at 0° reseal upon warming to 37° [49]. Across batches, entrapment efficiency, defined as the ratio of loaded, resealed ghosts to total RBCs, ranged from 30 – 80%. Although complete loading is ideal, it is not necessary for success of the sensor because

#146861 - $15.00 USD Received 2 May 2011; revised 17 Jun 2011; accepted 17 Jun 2011; published 22 Jun 2011

(1) the fluorescence signal is an integration of all resealed ghosts within the excitation volume and (2) unloaded RBCs do not contribute to the background signal. The final sensor design will include a reference fluorophore to account for variations in loading between batches, as well as in excitation and detection efficiencies.

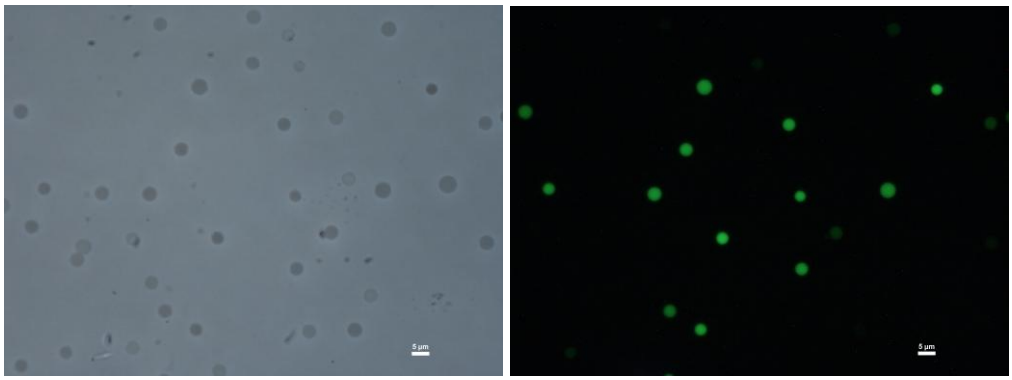

**(a)** **(b)**

Fig. 6. Representative (a) bright-field phase and (b) epifluorescence micrographs of resealed ghosts loaded with glycylglycine-FITC conjugate. (Scale bar represents 5 μm.)

## 4. Conclusions

RBCs offer a unique system for entrapping fluorescence-based sensing assays that protects the sensor from the damaging effects (e.g., biofouling) of the immune system. Furthermore, since normal RBCs live for 120 days, the red cell sensors have the potential to function for multiple months, significantly improving on current monitoring systems. In this work, we have shown that dye-loaded, resealed ghosts track changes in extracellular pH. Fluorescence intensity changes in response to pH were reversible, and the resealed ghost membranes were stable over the experimental time period. While it was shown that not all RBCs load during the procedure, complete loading, although a long-term goal, is not a requisite for success of this sensing system.

This platform technology offers the potential for a long-term, minimally-invasive method for monitoring blood analytes. Although the current system focuses on monitoring pH, the pH-sensitive dye could be replaced with a dye that is sensitive to a different analyte of interest, such as glucose. Since human RBCs rapidly transport glucose across the membrane, we expect that intracellular levels would track extracellular levels, similarly to the pH work shown here. Future work will focus on designing an RBC-based sensing system suitable for *in vivo* application through three specific avenues: (1) preparation of ghosts with near-normal Hb levels, thereby providing complete functionality *in vivo*; (2) incorporation of NIR dyes, where scattering and absorption of tissue/Hb are less significant, thereby increasing the excitation signal to the dye and emission signal to the detector, and (3) optimization of loading parameters to maximize loading homogeneity and efficiency, thereby maximizing the signal from the loaded ghosts.

## Acknowledgments

The authors would like to thank Dr. Timothy Glass for his useful advice throughout the project and Sina Amini for his assistance with the optical system. Sarah Ritter would like to thank the Department of Defense for their financial support through the National Defense Science and Engineering Graduate Fellowship. Dr. Mark Milanick presented a preliminary account of the idea of putting optical sensors inside red blood cells at the Red Cell Conferences, New Haven, Connecticut, 2006 and 2009.